

# Supplementary Material

## Quantification of Human Neuromuscular Function through Optogenetics

Olaia F. Vila<sup>1</sup>, Sebastien G.M. Uzel<sup>2,3</sup>, Stephen P. Ma<sup>1</sup>, Damian Williams<sup>4</sup>, Joey Pak<sup>1</sup>, Roger D. Kamm<sup>2</sup> and Gordana Vunjak-Novakovic<sup>1\*</sup>

<sup>1</sup>Department of Biomedical Engineering, Columbia University, New York, NY 10032, USA

<sup>2</sup>Department of Mechanical Engineering and Biological Engineering, Massachusetts Institute of Technology, Cambridge MA, USA

<sup>3</sup>School of Engineering and Applied Sciences, Wyss Institute for Biologically Inspired Engineering, Harvard University, Cambridge, MA 02138

<sup>4</sup>Columbia University Stem Cell Core Facility, Department of Rehabilitation and Regenerative Medicine, Columbia University, New York, NY 10032, USA

\*Correspondence to: [gv2131@columbia.edu](mailto:gv2131@columbia.edu)

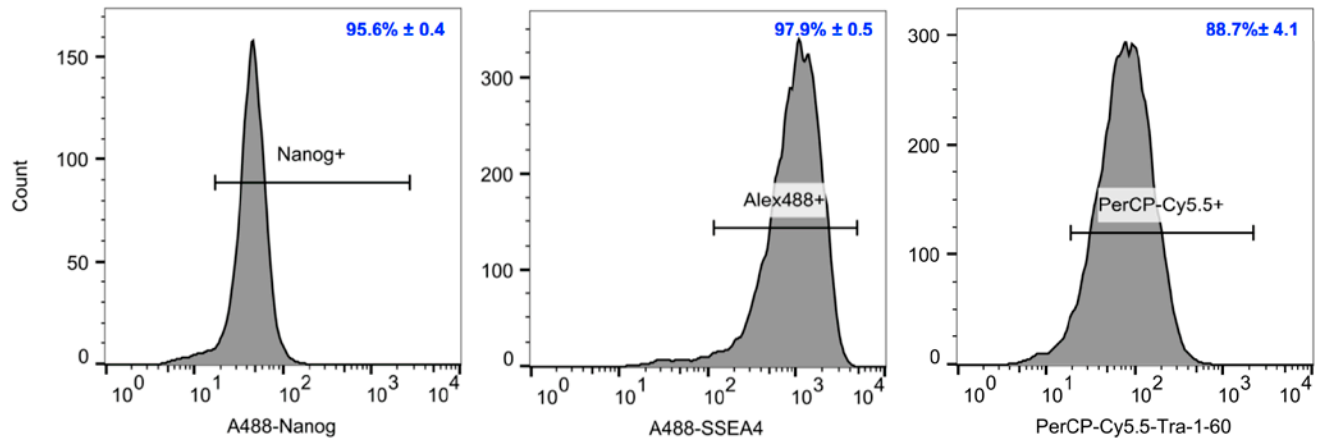


**Figure S1.** Expression of endogenous pluripotency markers Nanog, SSEA4 and Tra-1-60 in skeletal muscle-derived iPSCs cells at passage 3 after reprogramming with Sendai viruses.

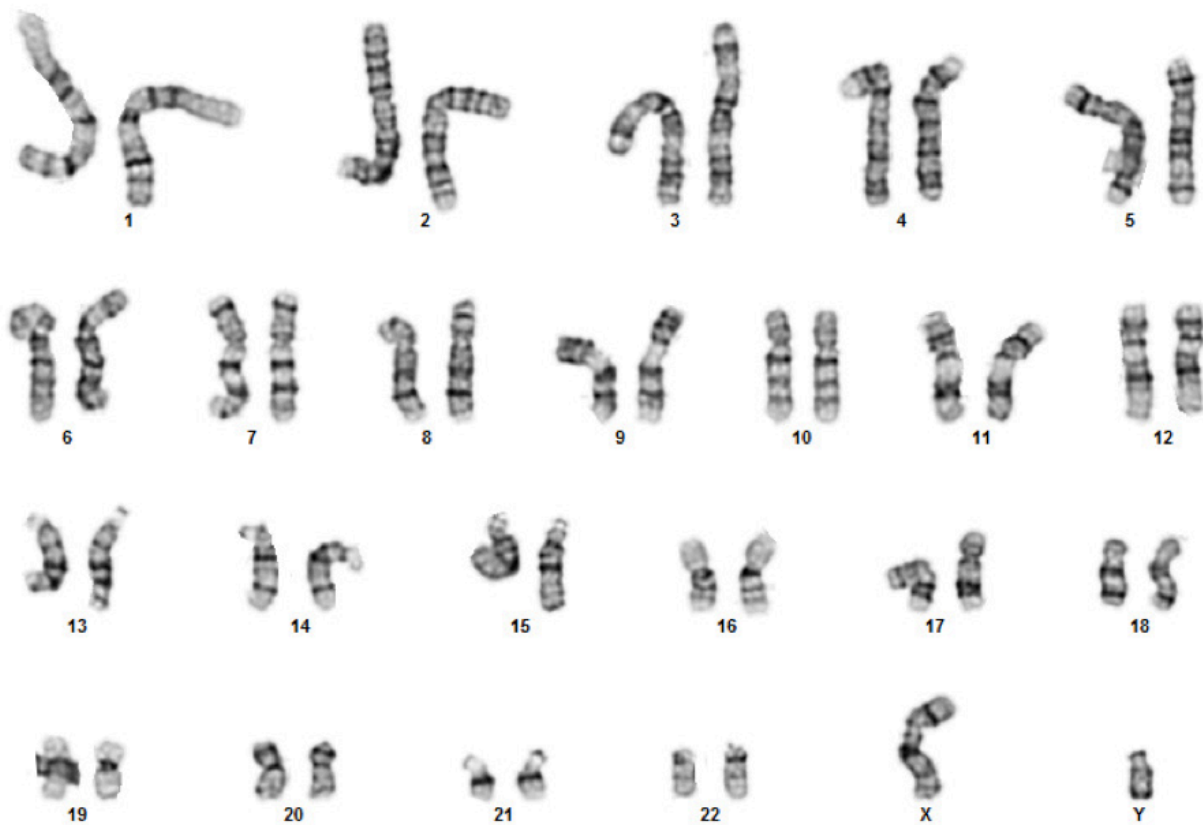


**Figure S2.** Representative cytogenetic analysis of the skeletal myoblast-derived iPSCs showing normal karyotype ( $n = 40$ ).

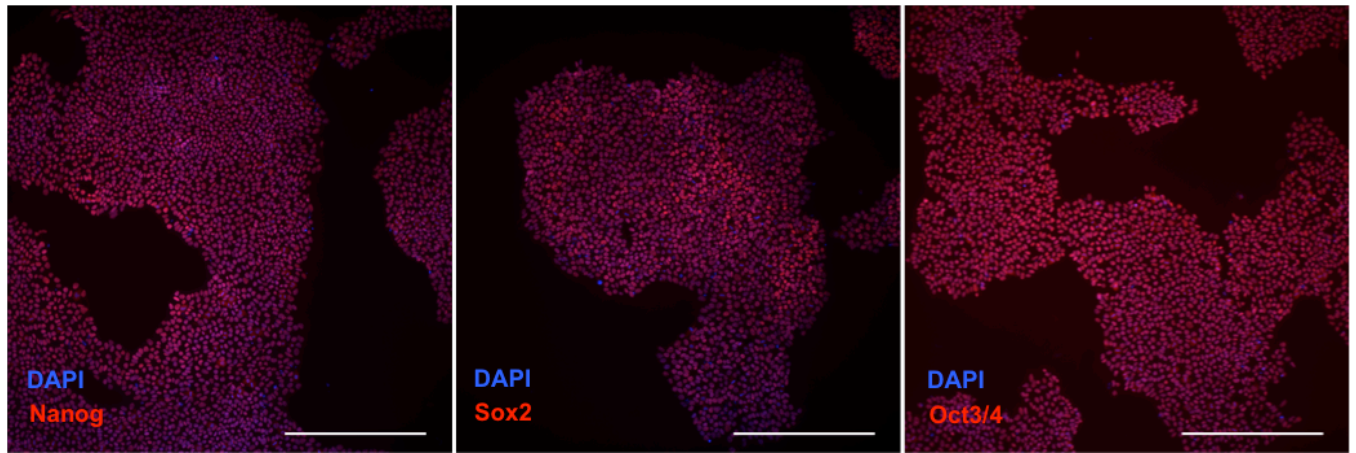


**Figure S3.** Immunofluorescence analysis of expression of pluripotency markers Nanog, Sox2 and Oct3/4 in skeletal muscle-derived iPSCs at passage 10. Scale bars: 500  $\mu$ m.

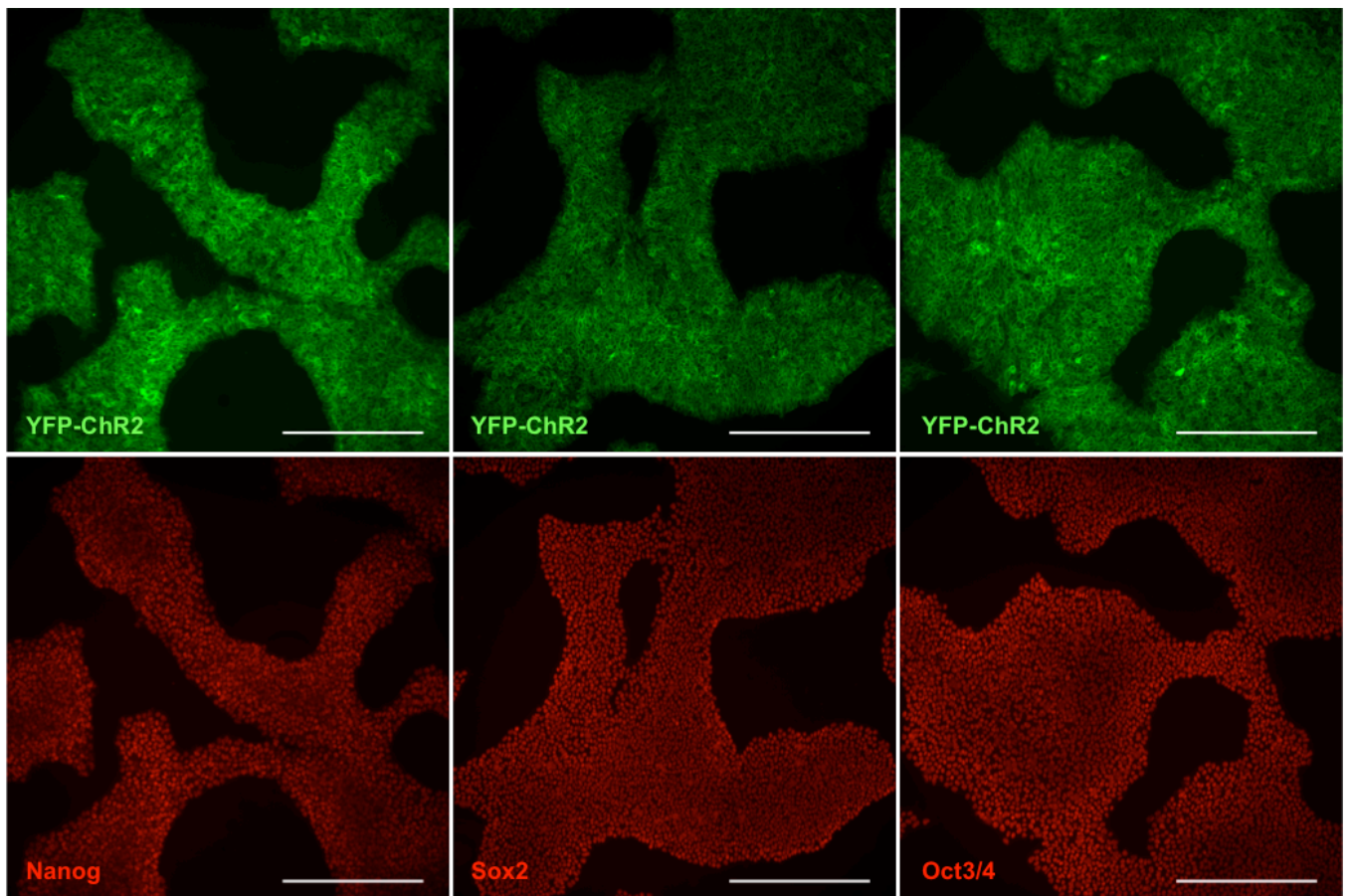


**Figure S4.** Immunofluorescence analysis of expression of pluripotency markers Nanog, Sox2 and Oct3/4 in skeletal muscle-derived iPSCs after introduction of the channelrhodopsin-2 gene (YFP-ChR2), passage 20. Scale bars: 500  $\mu$ m.

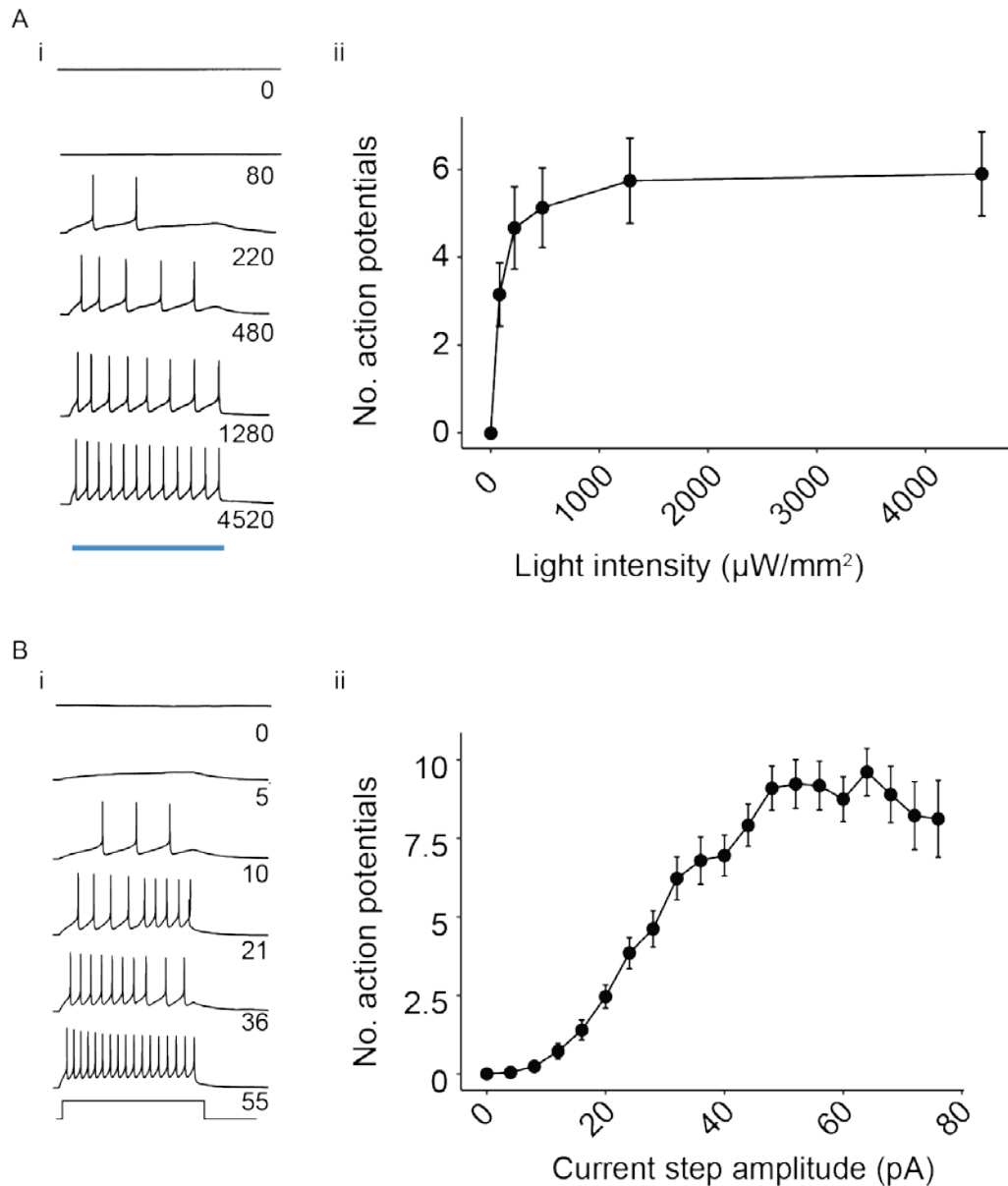


**Figure S5.** Light- and current-evoked action potentials in ChR2-expressing motor neurons derived from hiPSCs cells. **(A)** Light-evoked action potentials. **(i)** Representative membrane potential traces which show action potentials evoked by a 1 s light exposure at different intensities. Light intensities in  $\mu\text{W}/\text{mm}^2$  are indicated below each trace **(ii)** Graph showing the number of action potentials elicited by a 1 s exposure of light (shown in blue) at various intensities. **(B)** Current-evoked action potentials. **(i)** Membrane potential traces from the from the same cell shown in **A**. Action potentials were evoked by a 1 s current injection at incrementally increasing amplitudes. The amplitude of current injection is shown on the right of the trace. Traces are selected which closely match the action potential firing pattern evoked by light. The current injection step period is shown at the base of the column. **(ii)** Graph showing the number of action potentials elicited by a 1 s current step of different current injection amplitudes in the same cells shown in panel **A**. Data points represent the mean number of action potentials and  $n$  cells = 44 from 4 independent differentiations. Error bars=SEM.

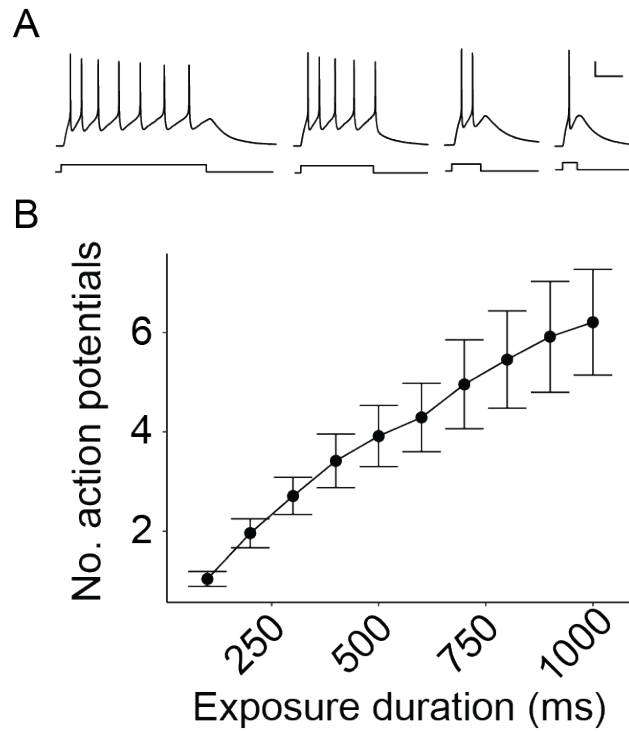


**Figure S6.** Action potentials evoked by different duration light exposure. A) Representative membrane potential recording from the same cell following exposure of 1000, 500, 200, and 100 ms 219 mW/mm<sup>2</sup> light. Bottom trace indicates periods of light exposure. Scale bar show 20 mV and 200 ms. B) Plot showing number of action potentials evoked by exposure to different durations of light.  $n = 24$  cells from 3 independent differentiations. Error bars=SEM.

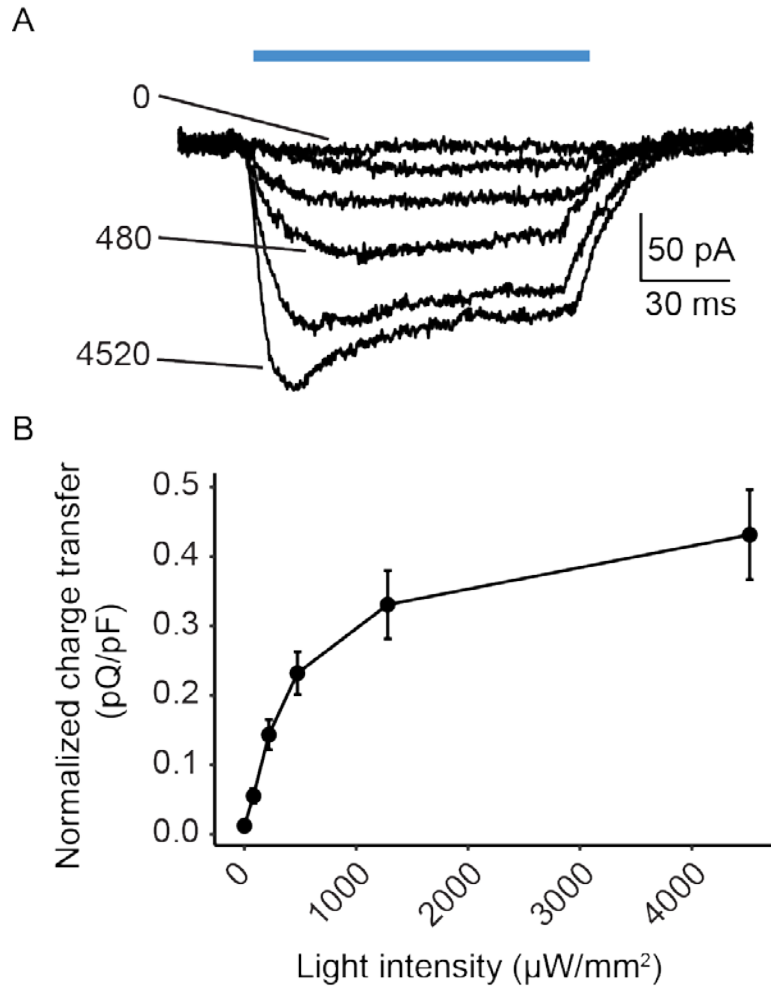


**Figure S7.** Light-evoked currents in ChR2-expressing iPSCs-derived neurons. **(A)** Voltage clamp recording showing membrane current traces from a neuron exposed to different intensities of light. For clarity, a subset of traces are labeled with the light intensity in  $\mu\text{W}/\text{mm}^2$ . The period of light exposure is indicated with a blue bar. **(B)** Plot showing the charge transfer normalized to cell capacitance during exposure to 100 ms light at different intensities. Data points represent the mean and SEM.  $n$  cells = 14.

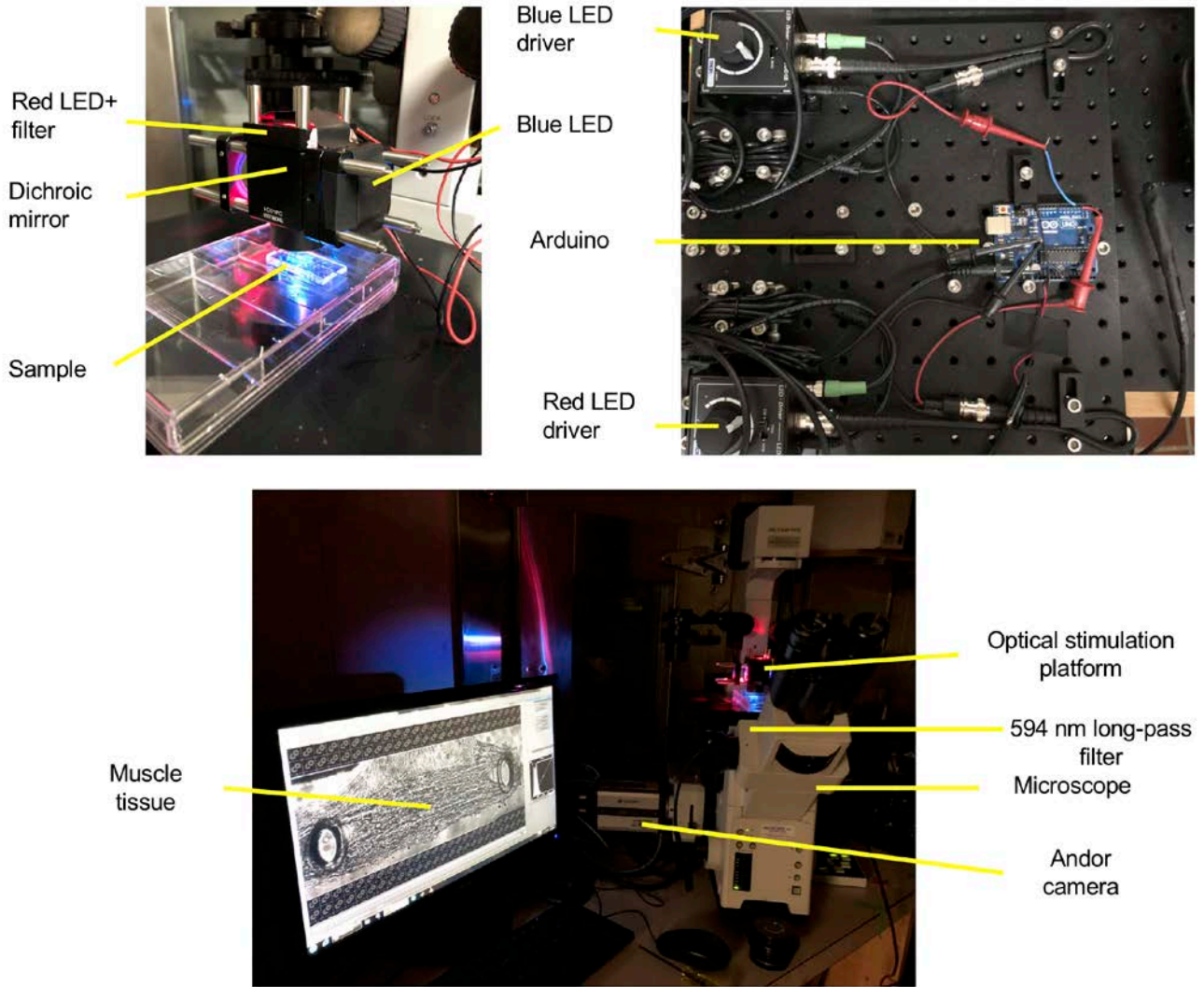


**Figure S8.** Optical stimulation platform comprising a 573nm dichroic mirror to couple red (627nm LED with a 594nm long-pass excitation filter) and blue (470nm LED with a 546nm short-pass excitation filter) light sources together. The LEDs were controlled with an Arduino Uno. For imaging, samples were placed on the stage of an Olympus FSX100 using the red LED from the optical platform as the source of brightfield illumination. A 594nm long-pass emission filter is placed on top of the microscope objective to filter out blue light for imaging.

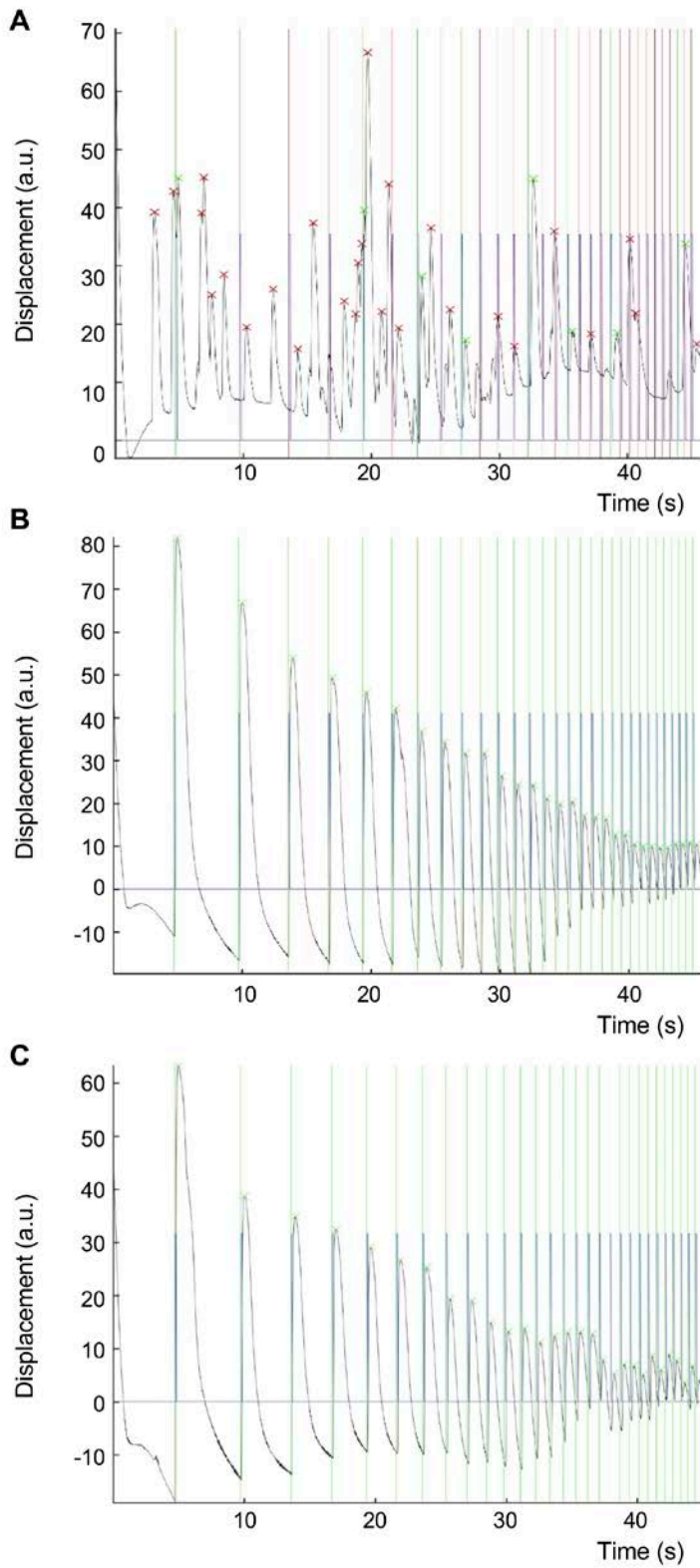


**Figure S9.** Tissue response to motoneuron stimulation with different pulse length durations. Contractility trace of a skeletal muscle tissue in response to motoneurons excitation with pulse lengths of 1 ms (**A**, score = 0.1), 10 ms (**B**, score = 1) or 100 ms (**C**, score = 1).

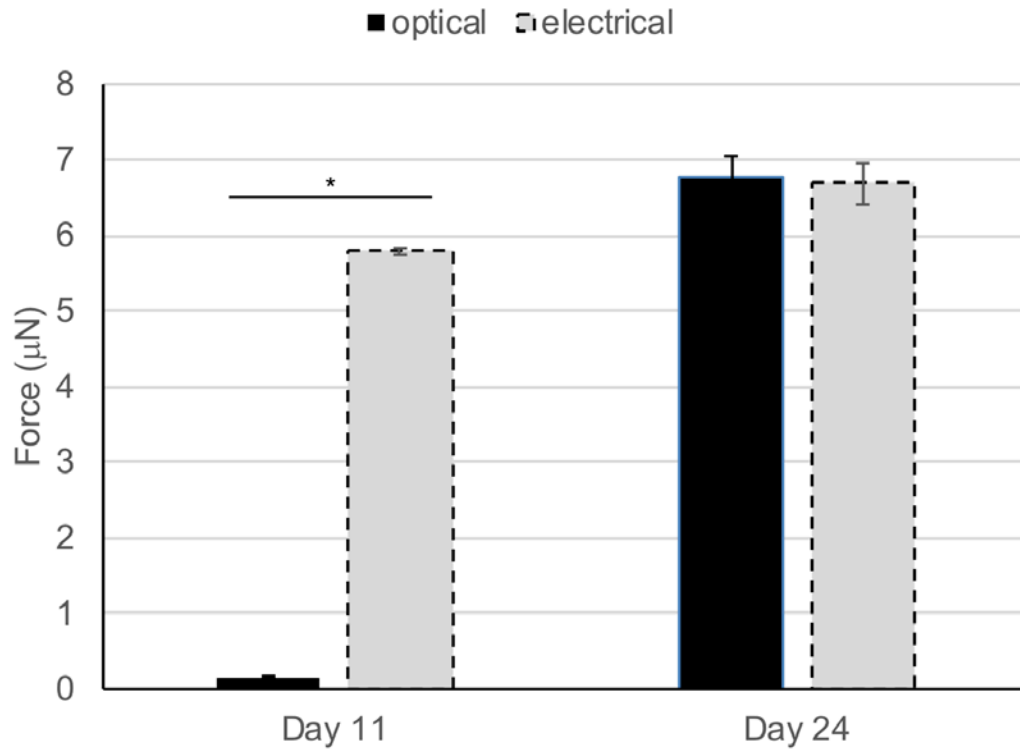


**Figure S10.** Calculation of forces generated by the skeletal muscle. Pillar displacement was measured and used to calculate the forces generated by the tissues after direct muscle stimulation with electrical currents and motoneuron stimulation with blue light. Measurements were performed at early (day 11) and late (day 24) stages (\* $p < 10^{-6}$ ,  $n = 3$ , error bars = SEM).

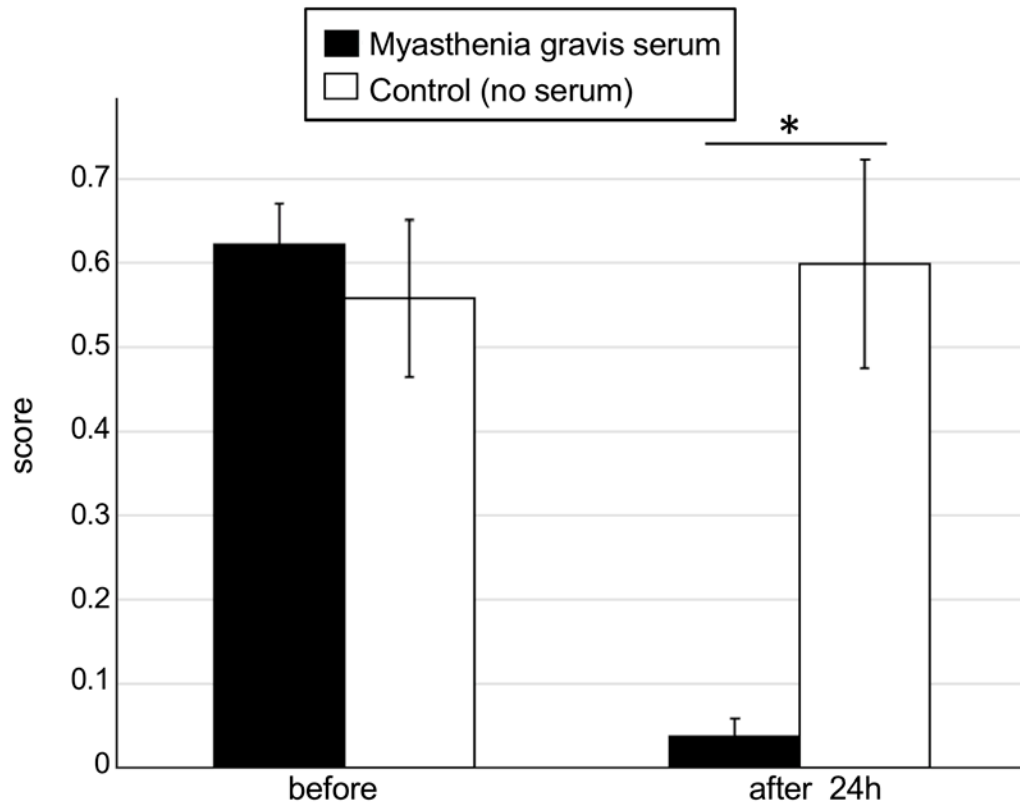


**Figure S11.** Quantification of NMJ function before and after 24h incubation with 10% of serum from MG patients ( $n = 12$ ; ANOVA  $F = 7 \cdot 10^{-5}$ ; error bars = SEM).

**Table S1. List of primary antibodies.**

<b>Antibody</b>	<b>Species and isotype</b>	<b>Manufacturer</b>	<b>Cat #</b>	<b>Dilution</b>
YPF	Rabbit IgG	Abcam	ab6556	1:1000
YPF mAb	Mouse IgG1	Abcam	ab1218	1:1000
$\alpha$ -actinin mAb	Mouse IgG1	Abcam	ab9465	1:100
NANOG mAb	Rabbit IgG	Cell Signaling	D73G4	1:200
OCT 3/4 mAb	Rabbit IgG	Cell Signaling	C30A3	1:200
SOX2 mAb	Rabbit IgG	Cell Signaling	D6D9	1:200
Desmin mAb	Mouse IgG1	Dako	M076029-2	1:100
MyoD	Rabbit IgG	Santa Cruz	sc-760	1:100
HB9 mAb	Mouse IgG1 $\kappa$	DSHB	81.5C10	1:100

**Table S2. List of secondary antibodies.**

<b>Antibody</b>	<b>Conjugation</b>	<b>Manufacturer</b>	<b>Cat #</b>	<b>Dilution</b>
Mouse IgG	AlexaFluor 488	ThermoFisher Scientific	A11001	1:1000
Rabbit IgG	AlexaFluor 488	ThermoFisher Scientific	A11008	1:1000
Mouse IgG	Alexa Fluor 555	ThermoFisher Scientific	A21422	1:1000
Rabbit IgG	Alexa Fluor 568	ThermoFisher Scientific	A11011	1:1000
Mouse IgG1 $\kappa$	AlexaFluor 488	ThermoFisher Scientific	A21127	1:500

**Table S3. List of conjugated antibodies for flow cytometry.**

<b>Antibody</b>	<b>Conjugation</b>	<b>Manufacturer</b>	<b>Cat #</b>	<b>Dilution</b>
TRA-1-6	Cy5.5	BD Biosciences	560173	1:50
SSEA4	AlexaFluor 488	BD Biosciences	560173	1:50
OCT4	AlexaFluor 488	BD Biosciences	560173	1:50

**Movie S1. Evaluation of NMJ functionality through optical stimulation and video processing.** Movie and contractility analysis of a functional tissue after 18 days in co-culture (day 30 for muscle). Blue blinker indicates blue light pulses (100 ms). Graph correlates light pulses (vertical lines) with tissue contractions (black trace). The ratio of effective pulses vs total number of pulses is used to score the tissues, in this case score = 1. Movie correspond to traces shown in **Figure 4A**.

**Movie S2. Presence of the optogenetic motoneuron is required for muscle response.** Optical stimulation of a muscle tissue in the absence of motoneurons at day 29. The movie was taken without filtering the blue light so the flashes could be observed.

**Movie S3. Evaluation of NMJ functionality after 20 min treatment with  $\alpha$ -bungarotoxin (BTX).** Movie and contractility analysis of same tissue from **Movie S1** after 20 min treatment with 5 $\mu$ g/ml BTX. The neurotoxin completely stops tissue responsiveness to light, as well as spontaneous contractions (score = 0). Movie correspond to traces shown in **Figure 4B**.

**Movies S4-6. Maturation of NMJs in a healthy tissue.** Movies and analysis of a representative tissue at day 9 (**Movie S4**, score = 0.06), day 11 (**Movie S5**, score = 0.12) and day16 (**Movie S6**, score = 0.71) post neuron-implantation demonstrate functional improvement of the NMJ. Movies correspond to traces shown in **Figure 5A-C**.

**Movies S7-9. Decreased functionality of NMJs after myasthenia gravis serum treatment and subsequent recovery.** Movie and analysis of a representative tissue before (**Movie S7**, score = 0.78), after 48 hours of treatment with 20% sera from myasthenia gravis patients (**Movie S8**, score = 0) and 48 hours after serum removal (**Movie S9**, score = 1) of the treatment

demonstrate blocking of the NMJ followed by complete recovery. Movies correspond to traces shown in **Figure 6A-C**.